Engineering Science and Technology, an International Journal 21 (2018) 679–691

HOSTED BY

Contents lists available at ScienceDirect

Engineering Science and Technology, an International Journal

journal homepage: www.elsevier.com/locate/jestch

Full Length Article

Path loss predictions for multi-transmitter radio propagation in VHF bands using Adaptive Neuro-Fuzzy Inference System

Nazmat T. Surajudeen-Bakinde [a], Nasir Faruk [b], Segun I. Popoola [c,*], Muhammed A. Salman [a], Abdulkarim A. Oloyede [b], Lukman A Olawoyin [b], Carlos T. Calafate [d]

[a] Department of Electrical and Electronics Engineering, University of Ilorin, Nigeria
[b] Department of Telecommunication Science, University of Ilorin, Ilorin, Nigeria
[c] Department of Electrical and Information Engineering, Covenant University, Ota, Nigeria
[d] Department of Computer Engineering, Technical University of Valencia (UPV), Valencia, Spain

ARTICLE INFO

Article history:
Received 19 February 2018
Revised 25 April 2018
Accepted 21 May 2018
Available online 30 May 2018

Keywords:
Path loss models
Adaptive Neuro-Fuzzy Inference System
Neural network
Radio wave propagation

ABSTRACT

Path loss prediction is an important process in radio network planning and optimization because it helps to understand the behaviour of radio waves in a specified propagation environment. Although several models are currently available for path loss predictions, the adoption of these models requires a trade-off between simplicity and accuracy. In this paper, a new path loss prediction model is developed based on an Adaptive Neuro-Fuzzy Inference System (ANFIS) for multi-transmitter radio propagation scenarios and applicable to the Very High Frequency (VHF) bands. Field measurements are performed along three driving routes used for testing within the urban environment in Ilorin, Kwara State, Nigeria, to obtain the strength values of radio signals received from three different transmitters. The transmitters propagate radio wave signals at 89.3 MHz, 103.5 MHz, and 203.25 MHz, respectively. A simple five-layer optimized ANFIS network structure is trained based on the back-propagation gradient descent algorithm so that given values of input variables (distance and frequency) are correctly mapped to corresponding path loss values. The adoption of the Pi membership function ensures better stability and faster convergence at minimum epoch. The developed ANFIS-based path loss model produced a low prediction error with Root Mean Square Error (RMSE), Standard Deviation Error (SDE), and correlation coefficient (R) values of 4.45 dB, 4.47 dB, and 0.92 respectively. When the ANFIS-based model was deployed for path loss predictions in a different but similar propagation scenario, it demonstrated a good generalization ability with RMSE, SDE, and R values of 4.46 dB, 4.49 dB, and 0.91, respectively. In conclusion, the proposed ANFIS-based path loss model offers desirable advantages in terms of simplicity, high prediction accuracy, and good generalization ability, all of them critical features for radio coverage estimation and interference feasibility studies during multi-transmitter radio network planning in the VHF bands.

1. Introduction

Propagation models, which can be empirical, semi-empirical or deterministic, are used in predicting the strength of a radio wave signal received at a given distance relative to the position of the base station transmitter. Path loss prediction models are used by radio network engineers to estimate the coverage area of a given transmitter. Empirical path loss models are widely used because they require less computational efforts. Also, detailed information about the physical and geometrical structures of the propagation environment are not required in the use of empirical path loss models. However, these models are not as accurate as deterministic models, especially when they are used in another environment that differs from the one where measurements were originally taken [1].

In previous works [2–8], the prediction accuracy of various empirical models have been investigated. These studies covered both urban and rural propagation environments in Nigeria. The results of the comparative analyses showed that empirical models are liable to high prediction errors. Although, research findings reported in [9–11] showed that some of the models with high performance can be tuned to minimize their prediction error and improve their prediction accuracy. However, the calibrated path loss models eventually become site-specific.

* Corresponding author.
E-mail addresses: segun.popoola@stu.edu.ng, segun.popoola@covenantuniversity.edu.ng (S.I. Popoola).
Peer review under responsibility of Karabuk University.

https://doi.org/10.1016/j.jestch.2018.05.013
2215-0986/

On the other hand, deterministic models are formulated based on theories and principles of physics, which are complex to implement and computationally expensive. Also, the prediction accuracy of deterministic path loss models is usually influenced by the accuracy and resolution of digital terrain model and topographical (or land use) database. In addition, it is sometimes necessary to fine-tune the path loss model even when a full and accurate database is available. This is done to guarantee model prediction accuracy [12].

Path loss predictions in rural areas were carried out successfully by Stocker and Landstorfer in [13], wherein an adaptive learning was used to develop a planning tool for mobile radio communication systems. In [14], a theoretical model and a neural network model were combined in the application of feed-forward Artificial Neural Network (ANN) for path loss predictions in an outdoor environment. The results obtained were compared to the prediction outputs of COST 231-Walfisch-Ikegami path loss model. In another related work by Eichie et al. [15], data were collected from selected rural and suburban areas of Minna, Niger State, Nigeria, and the measurement data were used in training ANN path loss model. The developed ANN-based path loss model was found to be better than Hata, Egli, COST 231, and Ericsson path loss models. Atmospheric parameters were used as inputs in developing two new models in [16]. It was observed that the developed model had an acceptable accuracy when compared to the measured values. In [17], the strengths of IS-95 pilot signal of a commercial Code Division Multiple Access (CDMA) mobile network was measured in a rural part of Western Australia, and the propagation measurements were used to train an ANN for path loss predictions. The proposed model, when compared to the ITU-R P.1546 and Okumura-Hata models, was found to be more efficient. In a related work, Neškovi'c et al. [18] proposed a prediction model based on feed forward neural networks for the mobile phone environment. The results obtained showed that the model is fast, accurate and reliable.

Benmus et al. [19] took measurements in Tripoli, Libya, and applied an ANN model to predict path loss in the Ultra-High Frequency (UHF) band. The results of the model, after evaluation and comparison, were found to be more accurate than the Hata model. In another research effort [20], very similar to the work done in this paper, an ANFIS-based path loss model was developed by training the network with field measurement data that were taken at 900 MHz in Harbiye, Province of Turkey, to predict path loss values at varying distances. There was a 15% increase in prediction accuracy for the ANFIS-based path loss model when its prediction outputs were compared to those of Bertoni-Walfisch path loss model. Angeles and Dadios [21] found Neural Network (NN) model to be the most efficient for path loss predictions in digital TV macro cells in the UHF band, when a comparative analysis was done in reference to the Free Space Loss (FSL) and Egli models. The prediction accuracy and generalization ability of ANN and Extreme Learning Machine (ELM) algorithms were investigated in [22,23].

Different Artificial Intelligence (AI) models have also been used to achieve high accuracy and better computational efficiency in path loss predictions [24,25]. Gupta and Sharma [26] employed the Fuzzy Logic (FL) model to predict path loss as a function of the path loss exponent in the fringe areas of the suburban region of Clementown and Dehradun. Path loss predictions using heuristic algorithms in urban macro cellular environments were done in [27]. To the best of our knowledge, the depth of the work done with respect to the application of ANFIS to path loss predictions in the Very High Frequency (VHF) bands is still very limited. The effectiveness of the NF model needs to be tested in view of the terrain peculiarities of the environment under investigation. Also, previous works in the literature that employed the ANFIS technique for path loss modeling only considered single transmitter propagation scenarios. In short, the capability of the ANFIS technique to model path loss predictions in urban environments at VHF bands has not been widely investigated for the multi-transmitter propagation use case in the context of tropical geographic terrains such as in Nigeria. Meanwhile, there seems to be a continuous growth in the deployment of wireless systems which operate in the VHF band. Hence, the need for this present study.

In this paper, a new path loss prediction model is developed for multiple transmitter radio propagation scenarios in VHF band using ANFIS. Field measurements are performed along three drive test survey routes within an urban environment in Ilorin, Kwara State, Nigeria, to obtain the strength values of radio signals received from three base station transmitters. The transmitters propagate radio wave signals at 89.3 MHz, 103.5 MHz, and 203.25 MHz, respectively. The Received Signal Strength (RSS) data obtained are calibrated to corresponding path loss values. A simple five-layer optimized ANFIS network structure is trained based on the back-propagation gradient descent algorithm such that given values of input variables (distance and frequency) are correctly mapped to corresponding path loss values. The complete dataset that contained all data instances of separation distance between transmitter and receiver, frequency of transmission, and path loss, is randomly divided into 75% training data subset, and 25% testing data subset. Measurement data obtained from propagation scenarios in the training data subset are used for model development and validation. The developed model is tested with measurement data that were collected from different but similar propagation scenarios within the urban environment. Model complexity and prediction accuracy are optimized using least square error approach. The ability of different membership functions (generalized, triangular, trapezoidal, Gaussian, and pi) to ensure good stability and fast convergence at minimum epoch were experimentally investigated. The prediction accuracy and generalization ability of the proposed ANFIS-based path loss model are evaluated based on the Mean Absolute Error (MAE), Mean Square Error (MSE), Root Mean Square Error (RMSE), Standard Deviation Error (SDE), and correlation coefficient (R), relative to the path loss values in training and testing data subsets, respectively. Finally, the prediction outputs of the developed ANFIS-based path loss model are compared with four popular empirical path loss models (Hata, COST 231, Egli, and ECC-33) to determine the optimal model for radio coverage estimation and interference feasibility studies during multi-transmitter radio network planning in the VHF bands.

2. Materials and methods

This section is divided into two parts: the first part describes the measurement procedure, and the second part explains the adaptive NF approach to path loss modelling in the VHF band.

2.1. Measurement campaign procedure

Field measurements were performed along three drive test survey routes within an urban environment in Ilorin, Kwara State, Nigeria (Longitude 4°36′25″E, Latitude 8°25′55″N), to obtain the strength values of radio signals received from three base station transmitters. The transmitters of the Nigerian Television Authority (NTA) Ilorin, UNILORIN FM, and Harmony FM propagate radio wave signals at 89.3 MHz, 103.5 MHz, and 203.25 MHz, respectively. Radio signals transmitted were received by a dedicated Agilent spectrum analyzer mode N9342C and the measured data were carefully logged. The receiver was properly positioned in a vehicle driven at an average speed of 40 km/hr to minimize Doppler Effects [28–30]. The spectrum analyzer has a Displayed Average Noise Level (DANL) of −164 dBm/Hz, being able to detect even very weak

signals. A whip retractable antenna (70 MHz–1 GHz), a Global Positioning System (GPS) receiver, and a dedicated memory stick for data storage, were coupled to the analyzer. The external GPS receiver was attached to the roof of the vehicle, while the spectrum analyzer was positioned inside the vehicle [31]. The system configuration parameters of the spectrum analyzer and detailed system parameters of the transmitters are presented in Table 1 and Table 2 respectively. Three measurement routes (R1, R2 and R3) were surveyed, with R1 having two to three-storey buildings densely distributed, characterized with hills, valleys and thick vegetation over the area, thereby fitting into an urban area description. R2 is characterized by a dense distribution of buildings, and so qualifies for suburban, while R3 spans from suburban to rural area because it is a very busy road characterized by a mix of hills and valleys within the area. Unlike the measurement results reported in [32,33], a multi-transmitter propagation scenario was investigated in this present study; therefore, a channel scanner was used. This allows the spectrum analyzer to provide a complete multi-frequency site survey, with logs of the received signal strength of various transmitters (up to 20 channels) along with the time, date and GPS coordinates into memory storage. The measurement commenced with the configuration of the spectrum analyzer, where all the transmitting frequencies of the selected VHF television transmitters were saved. The terrain elevation of a specific measurement route is the same for all the transmitters considered. This is because the receiver (Rx) travels along the same path for each of the three antennas. Hence, the Rx height is the same in each case. However, the clutter types along the wireless communication paths are different, as the transmitters are not co-located. The clutter types along the wireless communication paths are shown in Fig. 1(a). The measurements over the three base station transmitter were conducted simultaneously along each of the three routes (R1, R2 and R3), and the receiver obtained the signal strength from each transmitter with varying clutter type along the transmission path. This multi-transmitter set-up is different from the conventional method where the measurement is conducted for each transmitter along predefined routes. This new setup enables us to examine both the terrain and clutter effects simultaneously across the bands. This also helps us to isolate the clutter effects. Fig. 1(b) shows the routes of the complete measurement scenario for the Ilorin campaign.

Data pre-processing was undertaken where by the local mean received power was converted to path loss using Eq. (1). MicroCal origin 8.5 was used and un-weighted sliding average smoothing algorithm with 10 smooth points to smooth the data set. This removes small-scale fading while preserving the path loss and shadowing effects statistics. Also, a pick peaks tool (using a Bayesian second derivative) was also utilized to minimize the noise in the data. A total of 3946 unique data instances were obtained after proper data preprocessing. The complete data was randomly divided into 75% training data subset, and 25% testing data subset. The training data subset was used for ANFIS path loss model train-

Table 1
Configuration of N9342C Agilent Spectrum Analyzer.

N9342C Agilent Spectrum Analyzer (100 Hz–7 GHz)	
Displayed average noise level (DANL)	−164 dBm/Hz
Preamplifier	20 dB
Resolution bandwidth (RBW)	10 kHz
Impedance	50 Ω
Whip Antenna frequency	70 MHz–1 GHz
Whip antenna gain	2.51 dBi
Receiver height above the ground	1.5 m
GPS antenna frequency	L1 band

Table 2
Characteristics of the Broadcast Transmitters.

Transmitter Name	Location	Latitude	Longitude	Center Frequency (MHz)	Height (m)	Transmitter Power (KW)
UNILORIN	Ilorin	8° 29′ 21″ N	4° 40′ 28″ E	89.30	100	1.0
HARMONY	Ilorin	8° 21′ 56″ N	4° 43′ 18″ E	103.5	125	7.0
NTA, ILORIN	Ilorin	8° 25′ 55″ N	4° 36′ 25″ E	203.25	185	2.4

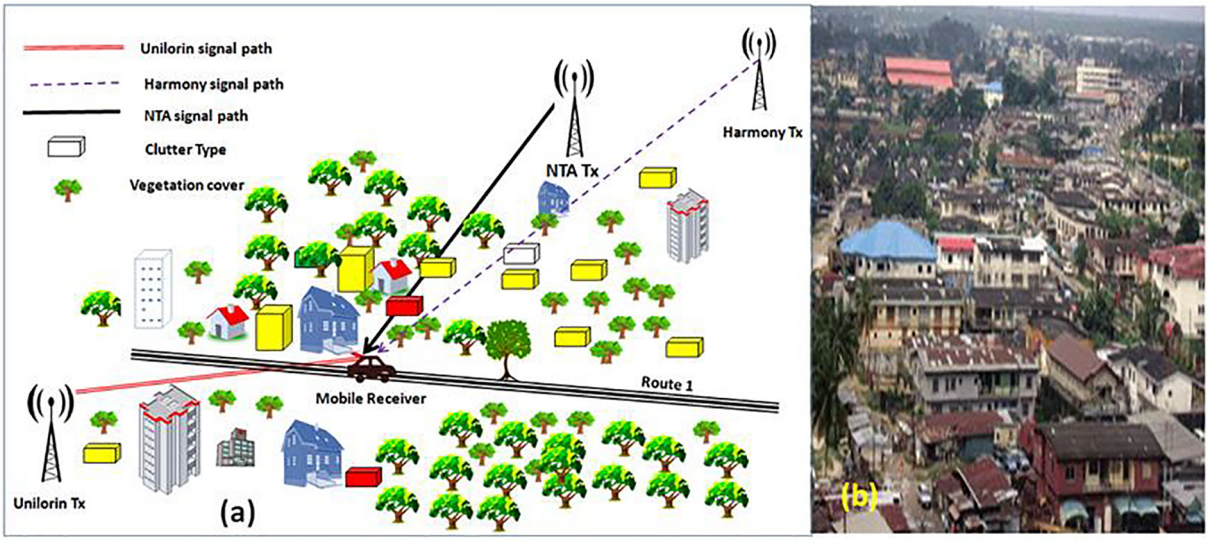

Fig. 1. Data collection for Ilorin, Kwara State, Nigeria (a) Multi-transmitter measurement scenario along route 1 showing the clutter types and (b) typical route within ancient part of Ilorin.

ing and development in MATLAB 2016a. The testing data subset, which were collected from different but similar propagation scenarios within the urban environment, and previously excluded from model training and development, was used to evaluate the prediction accuracy and generalization ability of the ANFIS path loss model. Training data and testing data do not contain the same data instances such that the two datasets represent different propagation scenarios.

$$Path\ Loss(dB) = Power_{transmitted} - Power_{received} \tag{1}$$

2.2. Prediction models

2.2.1. Neuro-Fuzzy (NF) model

The Neuro-Fuzzy modelling approach involves the use of expert knowledge to train a neural network structure to map a given set of input data correctly to their corresponding path loss values. In particular, it is a Fuzzy Inference System (FIS) which prepares the mapping of inputs to the respective outputs. The ANFIS method is not just a simulation method; the technique can actually be used for predicting values of a dependent variable based on a given set of values of independent variable(s). ANFIS techniques have been widely applied to solve prediction (or regression) problems in different fields of study [34–38]. In this study, the input variables that determine the output variable (path loss) are the separation distance between transmitter and receiver, and the frequency of transmission. The NF model structure consists of both the Fuzzy Logic (FL) and Artificial Neural Network (ANN), which complement one another in the development of mapping the supplied inputs to their corresponding outputs. The most significant reason for this combination is that the FL system makes use of the learning ability of the ANN. The most complex part of the FL technique is in deciding on the most suitable membership functions (generalized bell, Gaussian, triangular, trapezoidal, pi, etc.) to be adopted for the inputs, as well as generating the fuzzy rules (fuzzification) for the desired outputs. The membership function defines how each point in the input space (universe of discourse) is mapped to a membership value or degree of membership between 0 and 1. The input (antecedent) parameters are generated initially using a trial and error method. These parameters are therefore tuned by the learning ability of the ANN, which makes the errors reduction easier, as well as optimizing the output (consequent) parameters [39].

The structure consists of five layers, as shown in Fig. 2. The nodes in these layers are either fixed or adaptive. The adaptive nodes are symbolized by the square shapes, while the fixed nodes are represented by the circular shapes. To describe the structure, a first order Sugeno model has been used because the output is crisp, which does not require defuzzification. A Sugeno-based ANFIS has a rule of the form as given by Eqs. (2)–(4) [39]:

Rule 1: If x is A_1, and y is B_1, then:

$$f_1 = p_1x + q_1y + r_1 \tag{2}$$

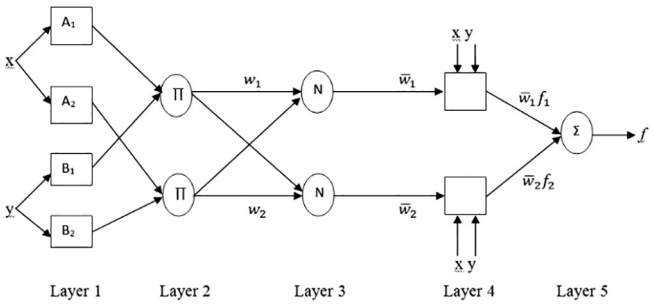

Fig. 2. ANFIS Structure.

Rule 2: If x is A_2, and y is B_2, then:

$$f_2 = p_2x + q_2y + r_2 \tag{3}$$

Layer 1: A node in this layer is adaptable, and is given as:

$$L_i^1 = \mu A_i(x), \quad i = 1,2 \tag{4}$$

x is the input to the *ith* node, A_i is the alterable language related to this node, and the membership function of A_i is $\mu A_i(x)$, usually taken as:

$$\mu A_i(x) = \frac{1}{1 + \left[\left(\frac{x-c}{a_i}\right)^2\right]^{b_i}} \tag{5}$$

$\{a_i, b_i, c_i\}$ forms a set called the antecedent parameters set. Eq. (5) represents the generalized bell membership function. Other membership functions used in the paper are the triangular, trapezoidal, Gaussian, and pi functions. Their model equations can be found in [32,40].

Layer 2: This layer is comprised of fixed nodes, and it solves the firing power w_i of a rule. The multiplication of the incoming signals is the output of each node, and is given by Eq. (6):

$$L_i^2 = w_i = \mu A_i(x) \times \mu B_i(y), \quad i = 1,2 \tag{6}$$

Layer 3: Each node is constant in this layer, with the output given by Eq. (7):

$$L_i^3 = \overline{w_i} = \frac{w_i}{\sum w_i}, \quad i = 1,2 \tag{7}$$

Layer 4: The adaptable output of this layer is given by Eq. (8):

$$L_i^4 = \overline{w_i} f_i = \overline{w_i}(p_ix + q_iy + r_i), \quad i = 1,2 \tag{8}$$

$\{p_i, q_i \text{ and } r_i\}$ also forms a set called the consequent parameters set, which are established by the least squares method.

Layer 5: The output of this layer is the summation of all incoming signals, and it is given by Eqs. (9) and (10):

$$L_i^5 = \sum_{i=1}^{2} \overline{w_i} f_i = \frac{\sum w_i f_i}{\sum w_i} \tag{9}$$

$$\begin{aligned} L_i^5 = z_p &= \sum_{i=1}^{2} \overline{w_i} f_i \\ &= (\overline{w_1}x)p_1 + (\overline{w_1}y)q_1 + (\overline{w_1})r_1 + (\overline{w_2}x)p_2 + (\overline{w_2}y)q_2 + (\overline{w_2})r_2 \end{aligned} \tag{10}$$

where z_p is the network predicted output.

A hybrid optimization method, which combines both the back propagation algorithm and a least square error method, was used for model network training. The output (consequent) parameters p_i, q_i and r_i are adjusted first by using the least squares algorithm, and those of input (antecedent) parameters a_i, b_i, and c_i by back propagating the faults from the output to the input until the training is completed.

The least squares estimate algorithm is obtained by rewriting Eq. (11) in matrix form [40]:

$$\begin{bmatrix} \overline{w_1}^{(1)}x^{(1)} & \overline{w_1}^{(1)}y^{(1)} & \overline{w_1}^{(1)} & \overline{w_2}^{(1)}x^{(1)} & \overline{w_2}^{(1)}y^{(1)} & \overline{w_2}^{(1)} \\ \overline{w_1}^{(2)}x^{(2)} & \overline{w_1}^{(2)}y^{(2)} & \overline{w_1}^{(2)} & \overline{w_2}^{(2)}x^{(2)} & \overline{w_2}^{(2)}y^{(2)} & \overline{w_2}^{(2)} \\ \vdots & \vdots & \vdots & \vdots & \vdots & \vdots \\ \overline{w_1}^{(n)}x^{(n)} & \overline{w_1}^{(n)}y^{(n)} & \overline{w_1}^{(n)} & \overline{w_2}^{(n)}x^{(n)} & \overline{w_2}^{(n)}y^{(n)} & \overline{w_2}^{(n)} \end{bmatrix} \begin{bmatrix} p_1 \\ q_1 \\ r_1 \\ p_2 \\ q_2 \\ r_2 \end{bmatrix} = \begin{bmatrix} z_p^{(1)} \\ z_p^{(2)} \\ \vdots \\ z_p^{(n)} \end{bmatrix} \tag{11}$$

n is the total number of training data (input/output) pairs, and $z_p^{(n)}$ are the network predicted outputs, where the consequent parameters $[p_1, q_1, r_1, p_2, q_2, r_2]^T$ are obtained using Eq. (12), and $z_d^{(n)}$ are the desired/measured outputs.

$$\begin{bmatrix} \overline{w_1}^{(1)}x^{(1)} & \overline{w_1}^{(1)}y^{(1)} & \overline{w_1}^{(1)} & \overline{w_2}^{(1)}x^{(1)} & \overline{w_2}^{(1)}y^{(1)} & \overline{w_2}^{(1)} \\ \overline{w_1}^{(2)}x^{(2)} & \overline{w_1}^{(2)}y^{(2)} & \overline{w_1}^{(2)} & \overline{w_2}^{(2)}x^{(2)} & \overline{w_2}^{(2)}y^{(2)} & \overline{w_2}^{(2)} \\ \vdots & \vdots & \vdots & \vdots & \vdots & \vdots \\ \overline{w_1}^{(n)}x^{(n)} & \overline{w_1}^{(n)}y^{(n)} & \overline{w_1}^{(n)} & \overline{w_2}^{(n)}x^{(n)} & \overline{w_2}^{(n)}y^{(n)} & \overline{w_2}^{(n)} \end{bmatrix}^{-1} \begin{bmatrix} z_d^{(1)} \\ z_d^{(2)} \\ \vdots \\ z_d^{(n)} \end{bmatrix} = \begin{bmatrix} p_1 \\ q_1 \\ r_1 \\ p_2 \\ q_2 \\ r_2 \end{bmatrix} \tag{12}$$

The errors between the desired and predicted outputs are propagated from the output layers to the input layers using the back propagation algorithm, which starts from Eq. (13) in order to update the synaptic weights [30]:

$$\overline{w_i}^{(k)}(M+1) = \overline{w_i}^{(k)}(M) + (z_d^{(k)} - z_p^{(k)}) \tag{13}$$

and the weight update for the input layer is given in Eq. (14)

$$w_i^{(k)}(M+1) = \begin{cases} w_i^{(k)}(M)x + \overline{w_i}^{(k)} \\ w_i^{(k)}(M)y + \overline{w_i}^{(k)} \end{cases} \tag{14}$$

where k is the input/output training pair, and M represents each layer starting from the output backwards.

2.2.2. Membership function (MF)

In the Membership Function (MF), μ refers to the degree or grade of membership of an element in a fuzzy set, and it must vary between 0 and 1. The most commonly used membership functions are the triangular, trapezoidal, generalized bell, Gaussian, and pi functions [34]. In this paper, we explore the impact of MF on the training RMSE for the model.

2.2.3. Empirical path loss models

The mathematical expressions for the path loss prediction models considered in the research work are presented in this section. In this study, the inclusion of existing path loss models is limited to popular empirical models because of their simplicity and lower computational requirements. Deterministic and semi-deterministic path loss models, such as ITU-R P.1411, ITU-R P.1546 and ITU-R P.1812 path loss models, require more detailed information about the propagation environment to guarantee a high prediction accuracy [41–43]. This paper seeks to identify an optimal model with desirable advantages of simplicity, high prediction accuracy, and good generalization ability that are required for radio coverage estimation and interference feasibility studies during multi-transmitter radio network planning in the VHF bands. Hence, the developed ANFIS-based path loss model was compared to only four empirical models (Hata, COST 231, Egli, and ECC-33) that met the inclusion criteria of simplicity and ease of use.

2.2.3.1. Hata model. Hata model may be used for path loss predictions within the frequency range of 150 MHz to 1500 MHz and distances up to 20 km. The height of the transmitter and receiver also varies between 30 and 200 m and 1–10 m, respectively. The mathematical expression for urban environments is given by Eq. (15):

$$PL_{Hata}(dB) = 69.55 + 26.16 \times \log(f) - 13.82 \times \log(h_t) - A(h_r) + (44.9 - 6.55 \times log h_t) \times \log(d) \tag{15}$$

where PL_{Hata} is the path loss (in dB), f is the operating frequency (in MHz), h_t is the height of the transmitter (in meters), h_r is the height of the receiver (in meters), d is the transmitter-receiver separation distance (in km), and $A(h_r)$ is the correction factor for the height of the receiver.

For a small and medium city, we have Eq. (16):

$$A(h_r) = (1.1 \times logf - 0.7)h_r - (1.56 \times logf - 0.8) \tag{16}$$

Whereas for a large city, we have Eq. (17):

$$A(h_r) = \begin{cases} 8.29 \times (log1.54 \times h_r)^2 - 1.1f \le 200MHz \\ 3.2 \times (log11.75 \times h_r)^2 - 4.97f \ge 200MHz \end{cases} \tag{17}$$

For sub-urban areas, we have Equation (18):

$$PL_{Hata}(suburban) = PL_{Hata}(urban) - 2 \times (\log(f/28))^2 - 5.4 \tag{18}$$

And for open areas, we have Eq. (19):

$$PL_{Hata}(open) = PL_{Hata}(urban) - 4.78 \times (logf)^2 + 18.33 \times \log(f) - 40.94 \tag{19}$$

2.2.3.2. Co-operative for scientific and technical research committee (COST) 231 model. The restriction of the Hata model in terms of frequency range, which has a maximum of 1500 MHz, inspired the COST 231 model. This model was developed as an extended version of the Hata model for frequencies up to 2 GHz, which accommodates the GSM 1800 MHz band, as well as distances up to 20 km. The mathematical expression is given by Eq. (20):

$$PL_{COST} = 46.3 + 33.9 \times \log(f) - 13.82 \times \log(h_t) - A(h_r) + (44.9 - 6.55 \times log h_t) \times \log(d) + C_m \tag{20}$$

where $C_m = 0$ dB for medium-sized cities and suburban areas, and 3 dB for metropolitan centers. $h_t, h_r, A(h_r)$, and $d$have the same ranges as defined for the Hata model.

2.2.3.3. Egli model. The Egli model is applicable for frequencies between 90 and 1000 MHz over irregular terrain, and remains valid for distances of less than 60 km. The path loss equation (in dB) for the model is given by Eq. (21):

$$PL_{Egli}(dB) = \begin{cases} 76.3 + 20 \times log(f) + 40 \times log(d) - 20 \times log(h_t) - 10 \times log(h_r) \\ \qquad for h_r \le 10m \\ 85.9 + 20 \times \log(f) + 40 \times \log(d) - 20 \times \log(h_t) - 10 \times \log(h_r) \\ \qquad for h_r \ge 10m \end{cases} \tag{21}$$

2.2.3.4. European communication committee (ECC-33) model. The ECC-33 model is an estimate of the measurements made by Okumura in the frequency range from 700 MHz to 3.5 GHz, and for distances between 1 and 10 km. The parameters of this model were modified to suit the fixed wireless systems (FWS) for urban and medium cities. The model was developed majorly for European cities, but it has found use in other countries as well, being given by Eq. (22):

$$PL_{ECC-33}(dB) = A_{fs} + M_{PL} - G_t - G_m \tag{22}$$

where A_{fs}, M_{PL}, G_t and G_m are the free space attenuation, median path loss, transmitter height gain factor, and mobile receiver height gain factor, respectively, and they are given by Eqs. (23)–(26):

$$A_{fs} = 92.4 + 20logd + 20logf \tag{23}$$

$$M_{PL} = 20.41 + 9.83logd + 7.894 \log f + 9.56(logf)^2 \tag{24}$$

$$G_t = \log(h_t/200) \times (13.958 + 5.8(logd)^2) \tag{25}$$

For a medium sized city we have:

$$G_m = (42.7 + 13.7 \times \log f) \times (logh_r - 0.585) \tag{26}$$

where f is in GHz, and d is in km.

3. Results and discussion

The strengths of the signals received by the dedicated Agilent spectrum analyzer mode N9342C were measured and recorded at varying distances as the vehicle moved away from the three transmitters that are considered in this study. The field measurements were performed along nine different drive test routes. A total of 4500 measurement points (i.e., 500 measurement points per route, multiplied by 9 drive test routes). The measurements taken along the nine drive test routes covered distance ranges of 0.044–10.026 km, 5.491–9.543 km, 7.081–8.353 km, 8.523–13.027 km, 9.525–11.437 km, 11.443–13.910 km, 13.530–22.435 km, 22.223–22.770 km, and 22.258–24.056 km, respectively.

Figs. 3–6 are the graphs of the measured and predicted path losses as a function of distance for the UNILORIN, NTA, and HARMONY transmitters, along R1. One route was followed in the data collection for each of the transmitters. From all the figures, it can be inferred that the prediction by the ANFIS model in all the three transmitters have the best performance, because of its similarity to the measured data, when they were compared to the four widely used empirical models: ECC-33, Egli, Hata and COST 231.

In R1 of UNILORIN transmitter, as shown in Fig. 3, ECC-33 is prone to overestimate results, except within a window of 0–1 km, where a good fitness value is achieved regarding the correlation with the measured path loss. Hata, COST 231 and Egli achieve values similar to the measured ones, except within the 4.5–5.5 km range, where Hata over-predicted the path loss. Under prediction of the path loss occurred within the distance range from 0 to 2 km for Hata, COST 231 and Egli. The same under prediction was observed within the range 9–10 km for the COST 231 and Egli models. ANFIS, on the other hand, has the same prediction trend for all measured values throughout the distance range considered.

In Fig. 4, the variation of path loss with distance for Route 3 is presented. The predictions of the four empirical models were superimposed on the measured loss. The Egli model underpredicted the path losses throughout the measurement route, except within the 9.0–9.8 km range, where the model prediction was good, being quite close to the measured path loss. COST 231 has a performance similar to Egli. Hata has an improved performance when compared to Egli and COST 231, because of its closeness to the actual measured values. Finally, the ANFIS model mimics the measured path loss throughout the whole range of distance considered.

In Fig. 5, the ANFIS model path loss is compared to the measured one and to four empirical path loss models for the NTA transmitter along R1. Notice that the ANFIS model predicts values that are very close to the measured ones throughout the whole path under analysis, while ECC 33 is in general prone to over predict values, especially in the range from 6.5 to 7.5 km. Egli under predicted the path loss throughout the whole coverage distance. On the other hand, Hata and COST 231 present nearly the same path loss, with evident under predictions within the 5.5–6. 5 km and 9.5–10 km ranges.

Fig. 6 depicts the result for the Harmony transmitter along R1. Path loss was over predicted by the COST 231 and Egli models for the distance range 15.1–15.8 km, while under prediction was

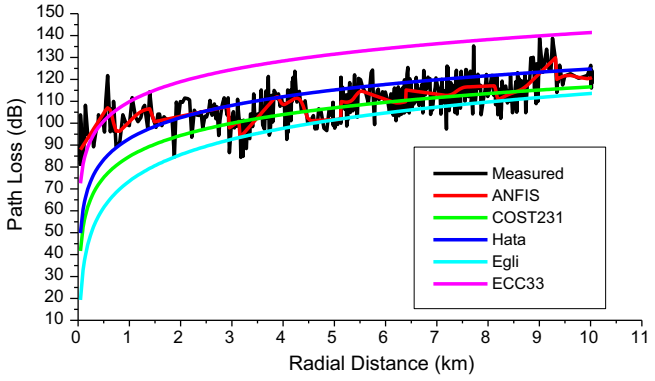

Fig. 3. Comparison of the ANFIS model path loss against the measured path loss and, other empirical models path loss along R1 for the UNILORIN Transmitter.

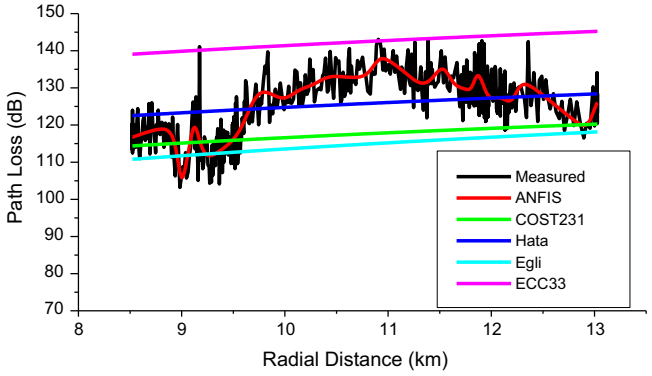

Fig. 4. Comparison of the ANFIS model path loss against the measured path loss, and other empirical models path loss, along R3 for the UNILORIN Transmitter.

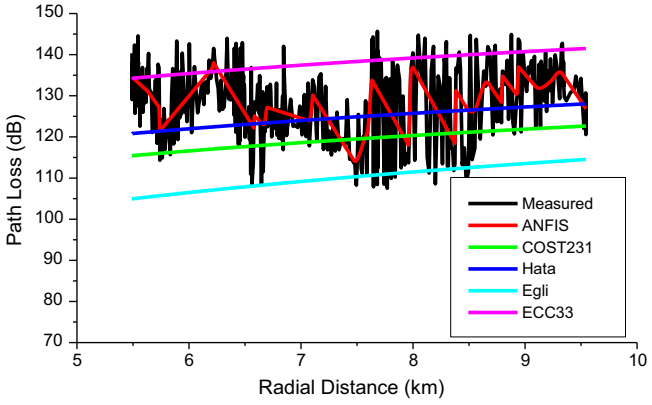

Fig. 5. Comparison of the ANFIS model path loss against the measured path loss, and other empirical models path loss, along R1 for the NTA Transmitter.

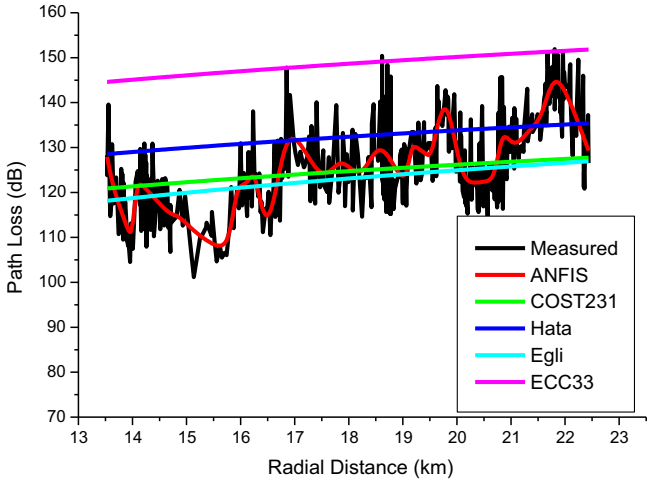

Fig. 6. Comparison of ANFIS model path loss against the measured path loss, and other empirical models path loss, along R1 for the Harmony Transmitter.

observed for the distance range 21–22.4 km. ECC-33 overpredicted values throughout the whole distance range considered, while Hata's performance was close to the measured prediction, especially from 16 to 22.5 km, but its path loss prediction was highly above the measured one from 14.8 to 16 km. As observed for the UNILORIN transmitters, the ANFIS model path loss values are identical to the measured path losses throughout the whole distance considered for the Harmony transmitter.

In Table 3, the statistical analysis of the error in terms of the RMSE for each model across the three target routes, and for the UNILORIN, NTA and HARMONY transmitters, are provided. A RMSE between 0 and 7 dB is considered acceptable for urban areas [26], although for typical suburban and rural areas, up to 10–15 dB can still be acceptable. The average RMSE values for the three routes and the three transmitters considered are the lowest, with values of 4.82 dB, 4.95 dB and 5.85 dB for UNILORIN, NTA and HARMONY transmitters, respectively. Notice that they all fall within the acceptable range for urban areas, where the transmitters are located. The next model with low average RMSE is Hata, which achieves 8.15 dB, 8.96 dB and 9.11 dB for the NTA, HARMONY and UNILORIN transmitters, respectively. ECC-33 has the highest average RMSE for the UNILORIN and HARMONY transmitters, with values of 18.63 dB and 21.19 dB, respectively.

In Table 4, the ANFIS model has the least mean error values for all the three transmitters – UNILORIN, NTA and HARMONY – considered along the three routes where the data were taken. This table further shows the accuracy of the ANFIS model in terms of path loss predictions when compared to the other four empirical models. The Egli model is next with very low mean error values throughout the three routes visited, and for the same three transmitters.

In Table 5, the maximum error performances of the three transmitters, UNILORIN, NTA and HARMONY, along the three routes (R1–R3) are depicted. Egli produced the highest error values, relative to the measured data, when used for path loss predictions along the three routes in this study

Table 6 shows the standard deviation Error (SDE) across all the ANFIS and the four empirical models, for UNILORIN, NTA and HARMONY transmitters. The SDE for R1 was highest for the UNILORIN transmitter in comparison to the two other transmitters, for all the models, which must have been due to high errors for these models along the concerned route. The HARMONY transmitter had the lowest SDE along R2 for all empirical models, except for the ANFIS model, which is quite high when compared to the others. The same performance trend observed for R2 is also applicable to R3 for the HARMONY transmitter, which has also the lowest SDE for all the models, except the ANFIS model.

In Fig. 7, the prediction error of the ANFIS model in terms of the radial distance is compared to all other empirical models for the UNILORIN transmitter along R1. It is observed from the graph that the ECC33 overestimated the path loss for the whole distance range covered. Egli, COST231 and Hata models underestimated the path loss within the distance range 0–3 km, having prediction errors of less than 0 dB, and they all converged to 0 dB at about 3.5 km. The path loss model has the lowest prediction errors of about -50 dB throughout the distance covered, except at a distance between 0 and 0.5 km, where the PE error was of 0 dB (the same as for the ANFIS model). The PE of the ANFIS model was of nearly

Table 3
RMSE Performance Metrics for the different models regarding the UNILORIN, NTA and Harmony Transmitters.

Models/Routes	UNILORN				NTA				HARMONY			
	R1	*R2*	*R3*	*Avg.*	*R1*	*R2*	*R3*	*Avg.*	*R1*	*R2*	*R3*	*Avg.*
ANFIS (dB)	5.71	4.16	4.60	4.82	7.10	3.82	3.94	4.95	5.87	5.46	6.21	5.85
COST 231 (dB)	13.39	12.54	11.51	12.48	13.14	9.56	7.49	10.06	8.85	9.68	10.19	9.57
Hata (dB)	12.39	7.07	7.87	9.11	9.79	6.41	8.24	8.15	10.66	8.24	7.99	8.96
Egli (dB)	19.74	16.22	13.58	16.51	21.21	16.22	11.24	16.22	9.04	10.17	10.68	9.96
ECC-33 (dB)	22.24	15.45	18.2	18.63	12.53	13.01	18.77	14.77	24.02	20.2	19.34	21.19

Table 4
Mean Error Performance Metrics for the different models regarding the VHF Transmitters.

Models/ Routes	UNILORN				NTA				HARMONY			
	R1	*R2*	*R3*	*Avg.*	*R1*	*R2*	*R3*	*Avg.*	*R1*	*R2*	*R3*	*Avg.*
ANFIS (dB)	1.04E−06	−5.68E−06	−1.78E−06	7.54E−06	−5.9E−05	1.82E−06	6.80E−06	−9.24E−06	−1.52E−05	1.04E−06	−5.68E−06	−1.78E−06
COST 231 (dB)	5.66	10.65	8.4	9.83	8.56	6.62	1.52	5.51	6.43	5.66	10.65	8.4
Hata (dB)	−2.48	−2.5	−0.25	−4.45	−3.17	−1.241	6.13	2.14	1.21	−2.48	−2.5	−0.25
Egli (dB)	−12.1	−14.7	−11.2	−19.25	−17.57	−14	−3.14	−6.31	−7.16	−12.1	−14.7	−11.2
ECC-33 (dB)	19.2	14	16.4	8.99	10.3	12.28	22.44	18.6	17.7	19.2	14	16.4

Table 5
Maximum Error Performance Metrics for the different models regarding the VHF Transmitters.

Models/Routes	UNILORN				NTA				HARMONY			
	R1	*R2*	*R3*	*Avg.*	*R1*	*R2*	*R3*	*Avg.*	*R1*	*R2*	*R3*	*Avg.*
ANFIS (dB)	18.61	14.786	25.105	20.96	25.2	17.29	21.0	15.82	23.3218	18.61	14.786	25.105
COST 231 (dB)	62.14	30.95	25.69	29.00	29.00	18.28	25.2	22.96	23.83	62.14	30.95	25.69
Hata (dB)	53.99	22.80	17.54	23.61	23.61	18.96	17.55	15.37	16.17	53.99	22.80	17.54
Egli (dB)	84.51	35.21	29.04	39.45	39.45	25.049	26.71	23.71	24.60	84.51	35.21	29.04
ECC-33 (dB)	31.25	6.31	0.914	10.18	10.18	32.45	45	39.84	−0.299	31.25	6.31	0.914

Table 6
Standard Deviation Error for the different models regarding the UNILORIN, NTA and HARMONY Transmitters.

Models/Routes	UNILORN				NTA				HARMONY			
	R1	*R2*	*R3*	*Avg.*	*R1*	*R2*	*R3*	*Avg.*	*R1*	*R2*	*R3*	*Avg.*
ANFIS (dB)	8.27	4.69	7.51	4.71	4.6	6.33	7.76	5.66	4.78	8.27	4.69	7.51
COST 231 (dB)	16.09	0.55	1.73	2.075	1.85	0.76	1.99	0.071	0.27	16.09	0.55	1.73
Hata (dB)	16.09	0.55	1.73	2.075	1.85	0.76	1.99	0.071	0.27	16.09	0.55	1.73
Egli (dB)	20.24	14.8	2.17	2.76	2.47	1.02	2.56	0.092	0.35	20.24	14.8	2.17
ECC-33 (dB)	14.98	14.8	1.81	2.083	1.86	0.77	2.09	0.076	0.29	14.98	14.8	1.81

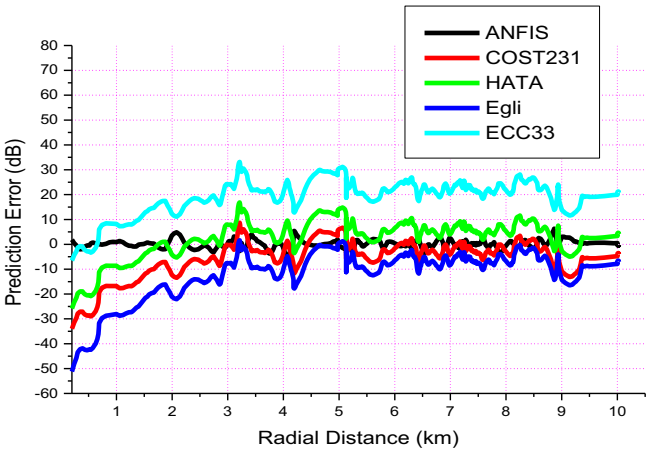

Fig. 7. Comparison of the ANFIS model prediction error with other empirical models prediction error for the UNILORIN Transmitter along Route 1.

0 dB throughout the distance covered for R1. The PE of Egli, COST 231 and Hata models show the same fluctuations, and follow the same behaviour as Egli, having the highest error among the three models throughout the whole distance covered. The ANFIS model has a constant PE of 0 dB throughout the 0–10 km range, with the Egli, COST231 and Hata models converging to 0 dB from 3.5 to10 km.

The impact of membership types and epoch size on RMSE is shown in Figs. 8–10, which are presented to show how the membership type provides stability to attain fast convergence with a minimum of epochs. In Fig. 8, as the number of epochs increases for the different types of membership functions for R1, UNILORIN

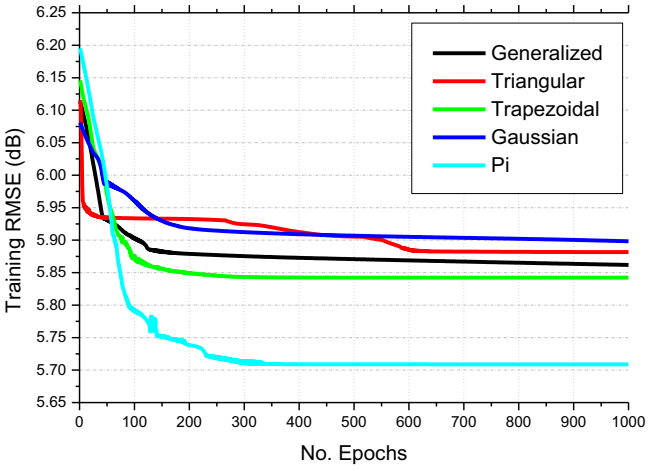

Fig. 8. Effects of the membership functions and the number of epochs on the training RMSE along R1 for the UNILORIN Transmitter.

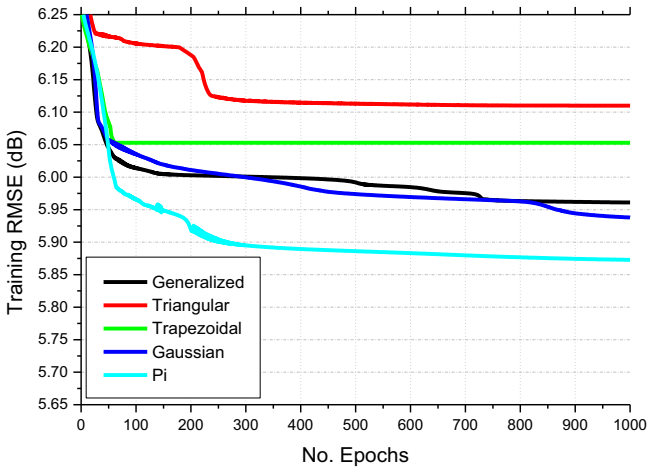

Fig. 9. Effects of the membership functions and the number of epochs on the training RMSE along R1 for the Harmony Transmitter.

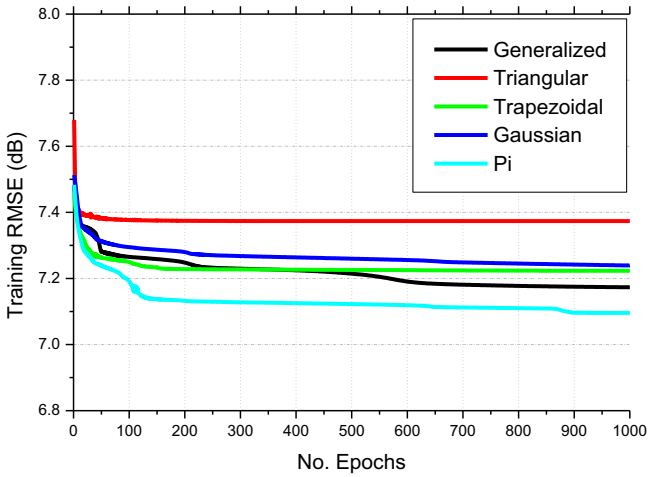

Fig. 10. Effects of membership functions and the number of epochs on the training RMSE along R1 for the NTA Transmitter.

transmitter, the RMSE also decreases. It is observed that Pi has the lowest RMSE for all the membership functions, and for all the epochs considered, stabilising at 5.70 dB from 300 to 1000 epochs. Trapezoidal is the next in line, with stable RMSE value of 5.85 dB from 200 to 1000 epochs. Gaussian and Triangular are both on the highest side for RMSE for all epochs considered.

In Fig. 9, the impact of the membership types and the epoch size on the RMSE for the Harmony transmitter along R1 is presented. Pi has the lowest RMSE, particularly from epoch size 100 to 1000, while the Generalized and Gaussian are trained in a similar

manner, with RMSE values falling within the 5.94–6.00 dB range. Trapezoidal achieves stable RMSE values of 6.05 dB from epochs of less than 100 up to 1000. Triangular achieves a very high RMSE (about 6.25 dB) from 0 epoch onwards, gradually decreasing to 6.13 dB where stability is observed, that is, from an epoch size of about 300 to 1000.

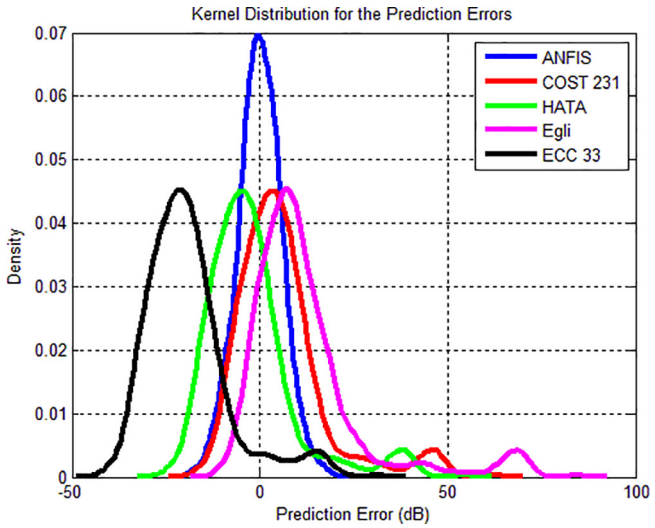

Fig. 11. Kernel distribution of the prediction errors for ANFIS and other empirical models along R1 for the UNILORIN transmitter.

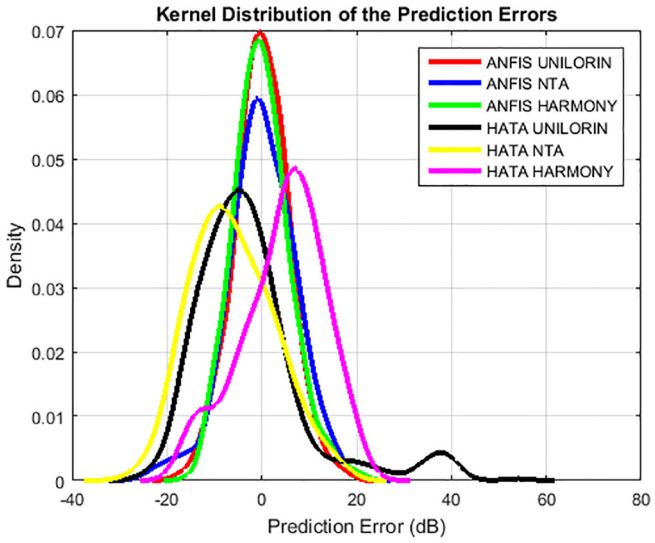

Fig. 12. Kernel distribution of the prediction errors for the ANFIS and HATA empirical models, for the NTA, UNILORIN and HARMONY transmitters along R1.

In Fig. 10, the impact of membership types and epoch size on RMSE for the NTA transmitter along Route 1 is presented. The RMSE for this transmitter, along the same R1 as for the two previous ones, is slightly different, while the Generalized, Trapezoidal and Gaussian functions achieve nearly the same values for all epoch sizes. Pi is observed to have the lowest RMSE, while Triangular maintained a very stable but high RMSE of 7.4 dB from 0 to 1000 epochs.

In Fig. 11, the response of the empirical models to clutter changes and radial distances is presented. It is observed that the clutter cover and radial distances do not affect the ANFIS model. The other empirical models are of very similar performance in their response to clutter cover and radial distances, whereas ANFIS is totally different in its response to the clutter cover.

In Fig. 12, along R1, the terrain elevation is the same, being that only the clutter along the communication path and the radial distance vary. It can be observed that both variables did not have significant effects on the ANFIS model, as both transmitters show similar shapes which are superimposed. However, slight amplitude offset for the NTA transmitter is noticeable. However, for the HATA model, a significant impact for the clutter and radial distance were observed. The error distribution for NTA and UNILORIN transmitters follows a similar curve, with slight offsets. A significant divergence for the HARMONY transmitter was also observed.

Large-scale fading represents the average reduction in signal power over a large distance, while small scale fading (i.e. rapid fluctuations of RSS within a short distance or period of time) is not considered in this work. In order to correctly account for large-scale fading alone, the mean path loss values were calculated by averaging the measurement data over a measurement track of 100 m. The prediction accuracy of the developed ANFIS-based path loss model was evaluated by comparing against the mean path loss data in the training data subset, and the prediction outputs of the Hata, COST 231, Egli, and ECC-33 path loss models. The performance results are presented in Table 7. The developed ANFIS-based path loss model produced the lowest prediction error, with MAE, MSE, RMSE, SDE, and R values of 3.386 dB, 19.844 dB, 4.455 dB, 4.470 dB, and 0.921, respectively.

The measured mean path loss values, and the prediction outputs of the ANFIS-based model, are plotted against separation distance, as shown in Figs. 13–15 for the training, testing, and complete datasets, respectively. The correlation between the measured average path loss values and the prediction outputs of the ANFIS-based model is depicted in Fig. 16. When the ANFIS-based model was deployed for path loss predictions in a different but similar propagation scenario, it demonstrated a good generalization ability, with MAE, MSE, RMSE, SDE, and R values of 3.545 dB, 19.840 dB, 4.454 dB, 4.489 dB, and 0.910, respectively. The generalization ability of the developed ANFIS-based path loss model was compared to the mean path loss data in the testing data subset, and to the prediction outputs of Hata, COST 231, Egli, and ECC-33 path loss models. The results of the statistical evaluation are presented in Table 8.

The developed ANFIS-based path loss model has been trained to map the values of the input variables (i.e. distance and frequency)

Table 7
Statistical evaluation of model prediction accuracy.

	MAE (dB)	MSE (dB)	RMSE (dB)	SDE (dB)	R
COST 231	7.437	102.818	10.140	8.595	0.779
Hata	6.480	74.814	8.650	8.466	0.776
Egli	11.074	216.467	14.713	10.694	0.768
ECC-33	18.075	380.922	19.517	8.207	0.776
ANFIS	3.386	19.844	4.455	4.470	0.921

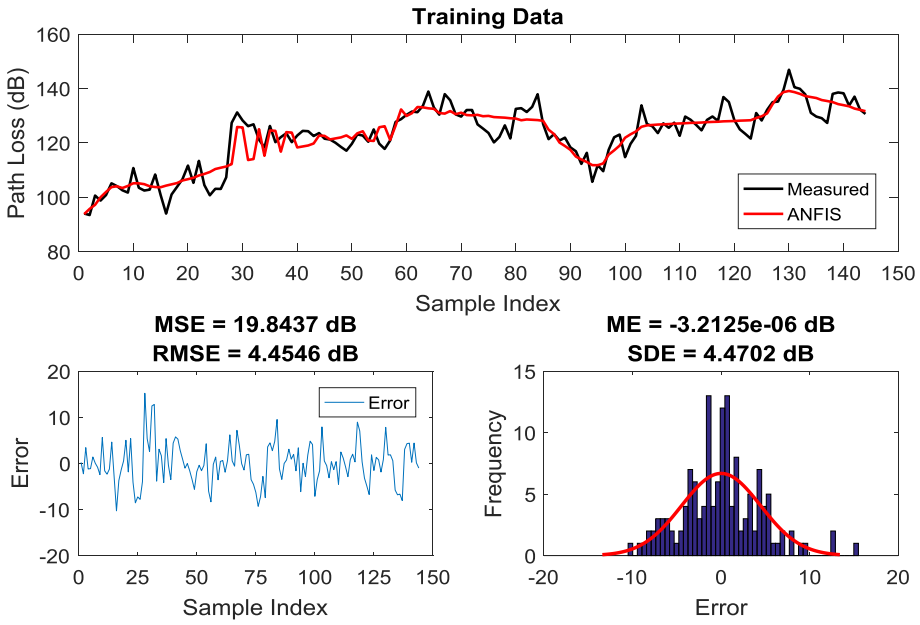

Fig. 13. Prediction performance of ANFIS-based path loss model.

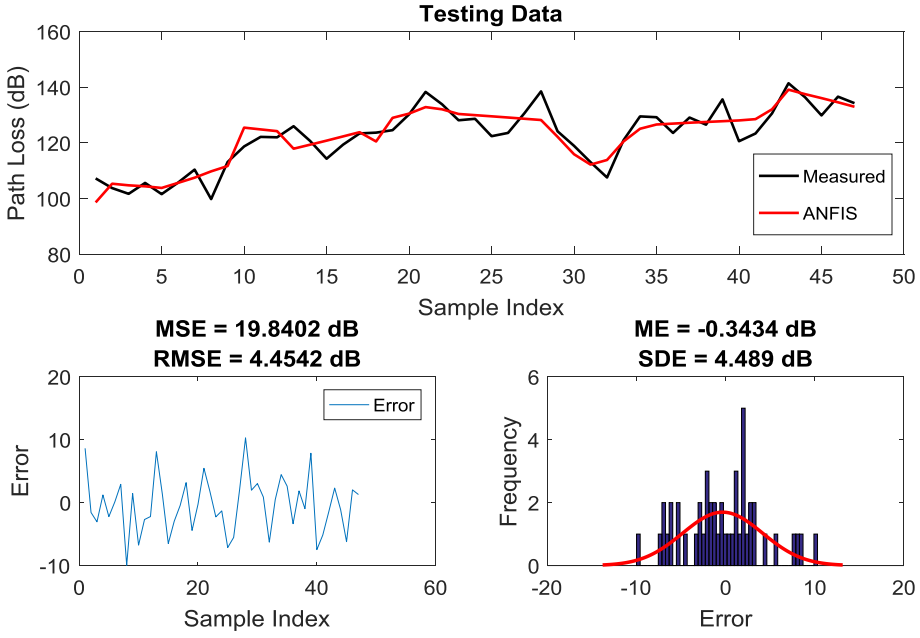

Fig. 14. Generalization performance of ANFIS-based path loss model.

to their respective path loss values. The trained model will produce the corresponding path loss value for any given distance in a different scenario, provided the geographic features in the new propagation environment are similar to those in the area where the training data were previously collected. Hence, the developed ANFIS model can be used to predict path loss for any given separation distance between transmitter and receiver, similar to what occurs for the Hata and other empirical path loss models. However, unlike other empirical models, which can be characterized by plain mathematical expressions, the trained ANFIS model acts as a "black-box" with the appropriate configurations of the input and output membership function parameters, rule antecedent, rule consequent, rule weight, and rule connection. The obtained configuration was encoded in the model network (*fis*) using the MATLAB programming language to accept the given values of separation distance and frequency of transmission as inputs, and produce path loss values as output. Path loss prediction can be performed using the *evalfis* function in MATLAB. Therefore, the developed ANFIS-based path loss model can simply be used to accurately predict path loss in the VHF band without any need for measurement data. Thus, measurement data is only needed for the training process. Thereafter, the already trained model can be deployed for path loss predictions in different propagation scenarios, and without the need to perform any field measurement.

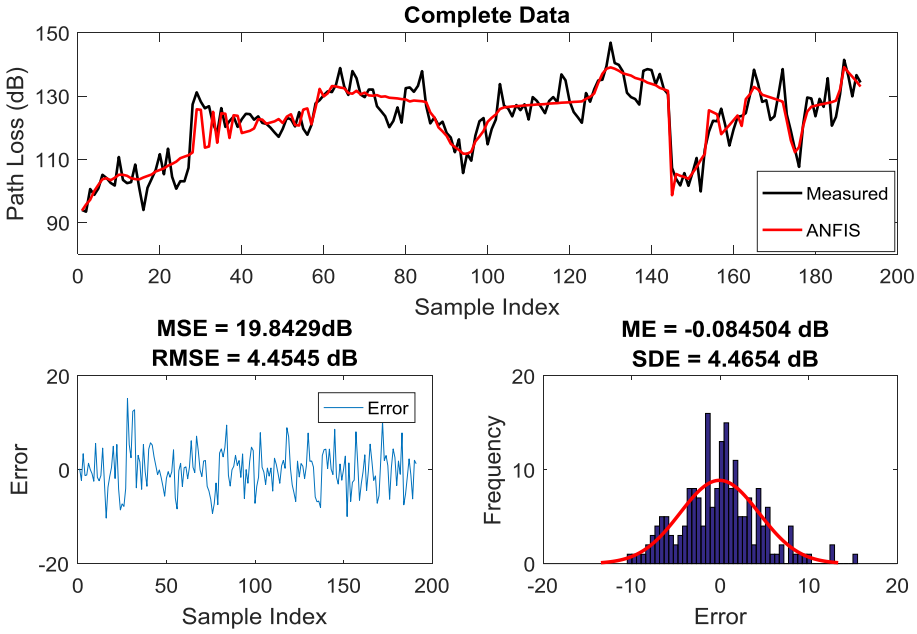

Fig. 15. General evaluation of ANFIS-based path loss model.

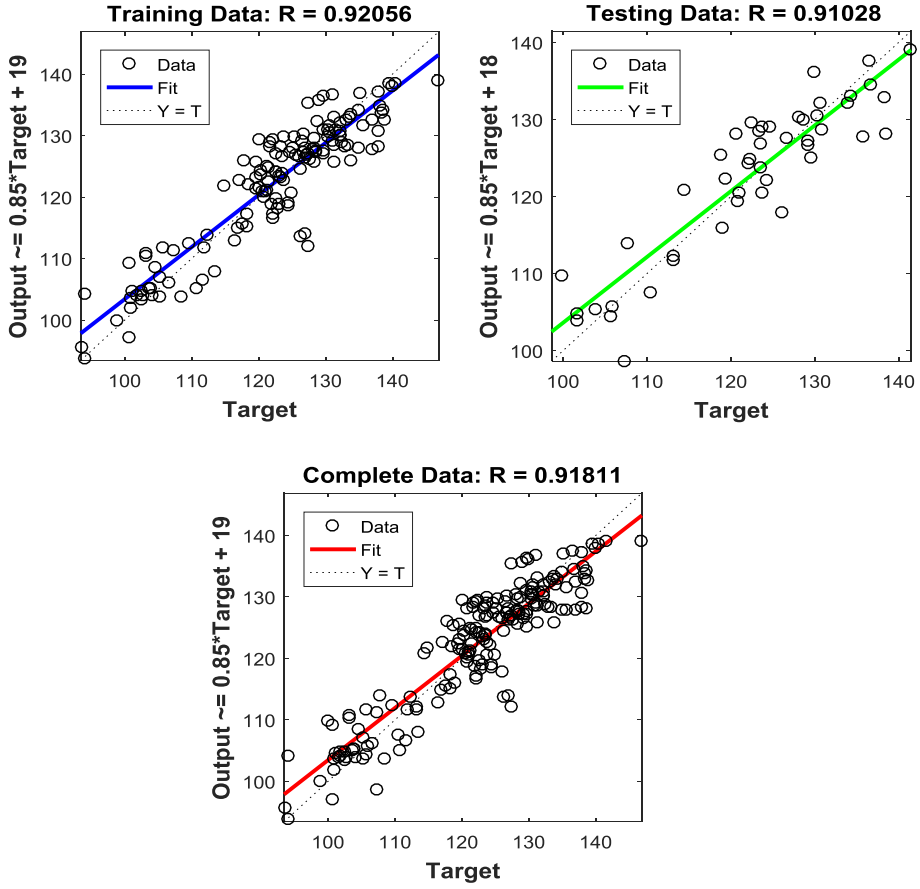

Fig. 16. *R* values of predicted path loss versus measured path loss.

In general, the developed ANFIS-based path loss model demonstrated the most desirable advantages in terms of simplicity, high prediction accuracy, and good generalization ability, that are required for radio coverage estimation and interference feasibility studies during multi-transmitter radio network planning in the VHF bands (Figs. 17 and 18).

Table 8
Statistical evaluation of model generalization ability.

	MAE (dB)	MSE (dB)	RMSE (dB)	SDE (dB)	R
COST 231	7.026	82.814	9.100	7.805	0.763
Hata	5.791	63.858	7.991	7.677	0.760
Egli	10.624	173.658	13.178	9.296	0.751
ECC-33	18.428	388.791	19.718	7.666	0.755
ANFIS	3.545	19.840	4.454	4.489	0.910

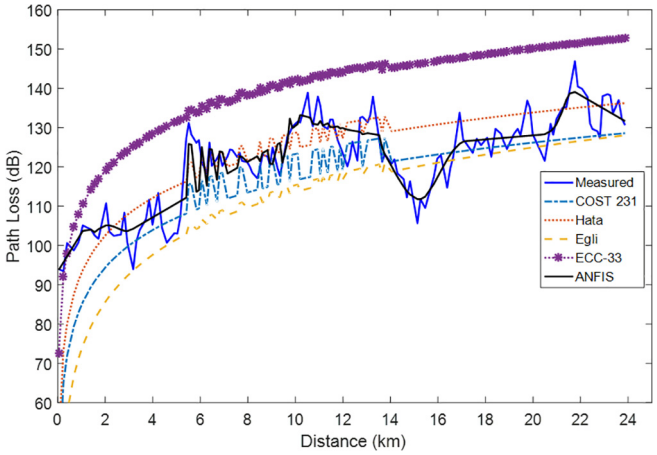

Fig. 17. Evaluation of prediction accuracy of Hata, COST 231, Egli, ECC-33, and ANFIS-based path loss models.

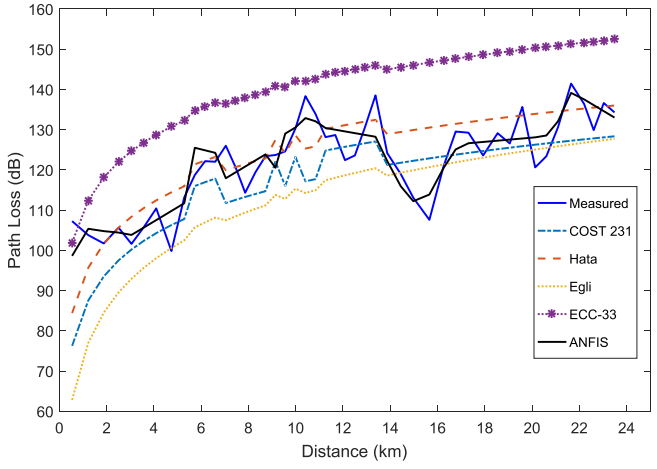

Fig. 18. Evaluation of generalization ability of Hata, COST 231, Egli, ECC-33, and ANFIS-based path loss models.

4. Conclusion

In this paper, a new path loss prediction model was developed for multiple transmitter radio propagation scenarios in the VHF bands using ANFIS. Extensive measurement campaigns were conducted along three routes within the urban environment of Ilorin, Kwara State, Nigeria. This was done using drive tests to obtain the strength values of radio signals received from three different transmitters at 89.3 MHz, 103.5 MHz, and 203.25 MHz, respectively. A simple five-layer optimized NF network was developed based on the back propagation gradient descent algorithm and least square errors to reduce the complexity and improve the accuracy of path loss predictions in VHF bands. A good stability and faster convergence was achieved with a minimum of epochs using the Pi membership function. It was observed that the clutter cover and radial distances do not significantly affect the performance of the developed ANFIS model. The developed ANFIS-based path loss model produced minimum prediction error with Root Mean Square Error (RMSE), Standard Deviation Error (SDE), and correlation coefficient (R) values of 4.45 dB, 4.47 dB, and 0.92 respectively. When the ANFIS-based model was deployed for path loss predictions in a different but similar propagation scenario, it demonstrated a good generalization ability with RMSE, SDE, and R values of 4.46 dB, 4.49 dB, and 0.91 respectively. In conclusion, the ANFIS model is able to deliver efficient path loss predictions required for radio coverage evaluation and interference feasibility studies in multi-transmitter radio network planning in the VHF bands.

Acknowledgement

The authors appreciate University of Ilorin for the purchase of the dedicated Agilent spectrum analyzer that was used for data measurement in this study.

References

[1] J.D. Parsons, The mobile radio propagation channel, Wiley, 2000.
[2] N. Faruk, Y.A. Adediran, A.A. Ayeni, Error Bounds of Empirical Path Loss Models at VHF/UHF Bands in Kwara State, Nigeria, IEEE Eurocon. 2013 (2013) 602–607.
[3] N. Faruk, A. Ayeni, Y.A. Adediran, On the study of empirical path loss models for accurate prediction of TV signal for secondary users, Progr. Electromagn. Res. B 49 (2013) 155–176.
[4] Jimoh, A.A., et al., Performance Analysis of Empirical Path Loss Models in Vhf & Uhf Bands. 2015 6th International Conference on Information and Communication Systems (Icics), 2015: p. 194-199.
[5] O.F. Oseni et al., Comparative analysis of received signal strength prediction models for radio network planning of GSM 900 MHz in Ilorin, Nigeria, Int. J. Innovative Technol. Exploring Eng. 4 (3) (2014) 45–50.
[6] O.F. Oseni et al., Radio frequency optimization of mobile networks in abeokuta, nigeria for improved quality of service, Int. J. Res. Eng. Technol. 3 (8) (2014) 174–180.
[7] S.I. Popoola, O.F. Oseni, Empirical path loss models for GSM network deployment in Makurdi, Nigeria, Int. Refereed J. Eng. Sci. 3 (6) (2014) 85–94.
[8] S.I. Popoola, O.F. Oseni, Performance evaluation of radio propagation models on GSM network in urban area of Lagos, Nigeria, Int. J. Sci. Eng. Res. 5 (6) (2014) 1212–1217.
[9] S.I. Popoola et al., Calibrating the Standard Path Loss Model for Urban Environments using Field Measurements and Geospatial Data, in: Lecture Notes in Engineering and Computer Science, Proceedings of The World Congress on Engineering, London, U.K., 2017, pp. 513–518.
[10] Popoola, S.I., et al., eds. Standard propagation model tuning for path loss predictions in built-up environments. International Conference on Computational Science and Its Applications. 2017, Springer. 363-375.
[11] N. Faruk et al., Improved path–loss model for predicting TV coverage for secondary access, Int. J. Wireless Mobile Comput. 7 (6) (2014) 565–576.
[12] N. Faruk et al., Clutter and terrain effects on path loss in the VHF/UHF bands, IET Microwaves Antennas Propag. 12 (1) (2017) 69–76.
[13] K. Stocker, F. Landstorfer, Empirical prediction of radiowave propagation by neural network simulator, Electronics Lett. 28 (8) (1992) 724–726.
[14] I. Popescu et al., ANN prediction models for outdoor environment. in Personal, Indoor and Mobile Radio Communications, 2006 IEEE 17th International Symposium, IEEE, 2006.
[15] J.O. Eichie et al., Comparative analysis of basic models and artificial neural network based model for path loss prediction, Progr. Electromagn. Res. M 61 (2017) 133–146.
[16] J.O. Eichie et al., Artificial Neural Network model for the determination of GSM Rxlevel from atmospheric parameters, Eng. Sci. Technol. Int. J. 20 (2) (2017) 795–804.

[17] E. Ostlin, H.-J. Zepernick, H. Suzuki, Macrocell path-loss prediction using artificial neural networks, IEEE Trans. Veh. Technol. 59 (6) (2010) 2735–2747.
[18] A. Neskovic, N. Neskovic, D. Paunovic, Indoor electric field level prediction model based on the artificial neural networks, IEEE Commun. Lett. 4 (6) (2000) 190–192.
[19] T.A. Benmus, R. Abboud, M.K. Shatter, Neural network approach to model the propagation path loss for great Tripoli area at 900, 1800, and 2100 MHz bands, Sciences and Techniques of Automatic Control and Computer Engineering (STA), 2015 16th International Conference on, IEEE, 2015.
[20] T.E. Dalkiliç, B.Y. Hanci, A. Apaydin, Fuzzy adaptive neural network approach to path loss prediction in urban areas at GSM-900 band, Turkish J. Electr. Eng. Computer Sci. 18 (6) (2010) 1077–1094.
[21] J.C.D. Angeles, E.P. Dadios, Neural network-based path loss prediction for digital TV macrocells, Humanoid, Nanotechnology, Information Technology, Communication and Control, Environment and Management (HNICEM), 2015 International Conference on, IEEE, 2015.
[22] S.I. Popoola, S. Misra, A.A. Atayero, Outdoor path loss predictions based on extreme learning machine, Wireless Pers. Commun. 99 (1) (2018) 441–460.
[23] S.I. Popoola et al., Optimal model for path loss predictions using feed-forward neural networks, Cogent Eng. 5 (1) (2018) 1444345.
[24] M.A. Salman et al., Adaptive Neuro-Fuzzy model for path loss prediction in the VHF band, Computing Networking and Informatics (ICCNI), 2017 International Conference on, IEEE, 2017.
[25] I.Y. Abdulrasheed et al., Kriging based model for path loss prediction in the VHF band, 2017 IEEE 3rd International Conference on Electro-Technology for National Development (NIGERCON), 2017.
[26] V. Gupta, S. Sharma, Secure Path Loss Prediction in Fringe Areas Using Fuzzy Logic Approach, Advances in Computing, Control, & Telecommunication Technologies, 2009. ACT'09. International Conference on, IEEE, 2009.
[27] Cruz, J.C.D. and F.S. Caluyo. Heuristic modelling of outdoor path loss for 9m, 3m and 1.5 m antenna at 677 MHz. in Cybernetics and Intelligent Systems (CIS), IEEE Conference on. 2013. IEEE.
[28] Popoola, S.I., et al., Statistical Evaluation of Quality of Service Offered by GSM Network Operators in Nigeria, in World Congress on Engineering and Computer Science. 2017, IAENG: San Francisco, USA. p. 69-73.
[29] S.I. Popoola, A.A. Atayero, N. Faruk, Received signal strength and local terrain profile data for radio network planning and optimization at GSM frequency bands, Data in Brief 16 (2018) 972–981.
[30] S.I. Popoola et al., Data on the key performance indicators for quality of service of GSM networks in Nigeria, Data in Brief 16 (2018) 914–928.
[31] Popoola, S.I., et al., Path loss dataset for modeling radio wave propagation in smart campus environment. Data in Brief, 2018.
[32] S.P. Sotiroudis et al., Application of a composite differential evolution algorithm in optimal neural network design for propagation path-loss prediction in mobile communication systems, IEEE Antennas Wirel, Propag. Lett. 12 (2013) 364–367.
[33] S.I. Popoola, A.A. Atayero, O.A. Popoola, Comparative assessment of data obtained using empirical models for path loss predictions in a university campus environment, Data in Brief 18 (2018) 380–393.
[34] M. Mostafaei, ANFIS models for prediction of biodiesel fuels cetane number using desirability function, Fuel 216 (2018) 665–672.
[35] B. Vakhshouri, S. Nejadi, Prediction of compressive strength of self-compacting concrete by ANFIS models, Neurocomputing 280 (2018) 13–22.
[36] M. Kumar et al., Artificial Neuro-Fuzzy Inference System (ANFIS) based validation of laccase production using RSM model, Biocatalysis Agric. Biotechnol. 14 (2018) 235–240.
[37] Y.-L. Zhang, J.-H. Lei, Prediction of laser cutting roughness in intelligent manufacturing mode based on ANFIS, Procedia Eng. 174 (2017) 82–89.
[38] A. Baghban et al., ANFIS modeling of rhamnolipid breakthrough curves on activated carbon, Chem. Eng. Res. Des. 126 (2017) 67–75.
[39] DasMahapatra, R. Optimal power control for cognitive radio in spectrum distribution using ANFIS. in Signal Processing, Informatics, Communication and Energy Systems (SPICES), 2015 IEEE International Conference on. 2015. IEEE.
[40] Sotiroudis, S.P., et al. Optimal Artificial Neural Network design for propagation path-loss prediction using adaptive evolutionary algorithms. in Antennas and Propagation (EuCAP), 2013 7th European Conference on. 2013. IEEE.
[41] E. ÖstlinOstlin, H. Suzuki, H.-J. Zepernick, Evaluation of the propagation model recommendation ITU-R P. 1546 for mobile services in rural Australia, IEEE Trans. Veh. Technol. 57 (1) (2008) 38–51.
[42] Ostlin, E., H. Zepernick, and H. Suzuki. Evaluation of the new semi-terrain based propagation model Recommendation ITU-R P. 1546. in Vehicular Technology Conference, 2003. VTC 2003-Fall. 2003 IEEE 58th. 2003. IEEE.
[43] F.M. da Costa, L.A.R. Ramirez, M.H.C. Dias, Analysis of ITU-R VHF/UHF propagation prediction methods performance on irregular terrains covered by forest, Antennas & Propagation, IET Microwaves, 2018.